ELSEVIER

Biophysical Chemistry 99 (2002) 99–106

Biophysical Chemistry

www.elsevier.com/locate/bpc

Interaction of low-molecular-weight chitosan with mimic membrane studied by electrochemical methods and surface plasmon resonance

Fan Yang, Xiaoqiang Cui, Xiurong Yang*

State Key Laboratory of Electroanalytical Chemistry and National Analytical Research Center of Electrochemistry and Spectroscopy, Changchun Institute of Applied Chemistry, Chinese Academy of Sciences, Changchun, Jilin 130022, PR China

Received 7 February 2002; received in revised form 7 May 2002; accepted 10 May 2002

Abstract

Chitosan has shown its potential as a non-viral gene carrier and an adsorption enhancer for subsequent drug delivery to cells. These results showed that chitosan acted as a membrane perturbant. However, there is currently a lack of direct experimental evidence of this membrane perturbance effect, especially for chitosans with low molecular weight (LMW). In this report, the interaction between a lipid (didodecyl dimethylammonium bromide; DDAB) bilayer and chitosan with molecular weight (MW) of 4200 Da was studied with cyclic voltammetry (CV), electrochemical impedance spectroscopy and surface plasmon resonance (SPR). A lipid bilayer was formed by fusion of oppositely charged lipid vesicles on a mercaptopropionic acid (MPA)-modified gold surface to mimic a cell membrane. The results showed that the LMW chitosan could disrupt the lipid bilayer, and the effect seemed to be in a concentration-dependent manner.

Keywords: Low-molecular-weight chitosan; Lipid bilayer; Interaction; Cyclic voltammetry; Electrochemical impedance spectroscopy; Surface plasmon resonance

1. Introduction

Chitosan is a typical biological macromolecule derived from crustacean shells and has several applications in drug development, obesity control, tissue engineering, etc. [1]. Chitosan consists of polymeric 1→4 linked 2-amino-2-deoxyl-β-D-glucose, but its preparation and batches vary with respect to its degree of deacetylation and polymerization. Many derivatives, such as *N*-sulfonyl chitosan, and salts, such as chitosan lactate, with altered physicochemical properties can also be prepared.

Chitosan has been used as a bioadhesive and permeabilizer in pharmaceutical applications. [2] It is an ideal candidate for mucosal drug delivery. The co-administration of drugs and chitosan enhances the transcellular and paracellular transport of drugs across the mucosal epithelium [3]. Chitosan has also created significant interest in

*Corresponding author. Tel./fax: +86-431-5689711.
E-mail address: xryang@ns.ciac.jl.cn (X. Yang).

0301-4622/02/$ - see front matter
PII: S0301-4622(02)00134-5

biomedical applications due to its biodegradation, biocompatibility and bioactivities, such as antimicrobial activity and wound-healing acceleration [4,5]. In recent years, several studies have shown the potential use of chitosan in a DNA delivery system. Chitosans can form complex nanoparticles with recombinant DNA, which could provide an effective means for delivering genes into cells. [6–9]. These studies showed that chitosan–DNA nanoparticles overcame the cell membrane barrier [6] and induced gene expression in the absence of ligands on the nanoparticle surface [8]. Chitosan also affected the transfection efficiency of complexed DNA when the target cell was incubated with nanoparticles in the presence of chitosan [10].

All the studies implied that chitosans might have a disturbance effect on the cell membrane. The chitosans previously used were of relatively large molecular weight and in most cases were used at acidic pH. Richardson et al. [11] reported the potential of LMW chitosan as a DNA delivery system. The LMW chitosans were neither toxic nor hemolytic, and could complex DNA and protect against nuclease degradation. They can be administered intravenously.

So far, little direct experimental evidence of the interaction of chitosan with the cell membrane is available. In recent years, supported lipid bilayer membranes (s-BLM) have been used to mimic the properties of the cell membrane [12–16]. Here we have studied the interaction of LMW chitosan with s-BLM by electrochemical methods and surface plasmon resonance. A self-assembled monolayer of mercaptopropionic acid (MPA) was developed on the bare gold surface of an Autolab electrochemical surface plasmon resonance (ESPR) sensor disc. A lipid bilayer was then formed on the surface by electrostatic adsorption. Chitosan with a molecular weight of 4200 Da was used to study its interaction with the lipid bilayer.

2. Experimental

2.1. Reagents

Chitosan with a molecular weight of 4200 Da (degree of deacetylation 90%) was purchased from Haidebei (Jinan, China). 2-Mercaptopropionic acid and didodecyl dimethylammonium bromide were from Acros (Belgium). Chloroform was from Sigma (USA). All other chemicals were of analytical grade and used as received. Highly purified 18.2 MΩ distilled water was obtained from an ultrapure water purification system (Mini-Q Plus, Millipore Inc) and was used in the preparation of all solutions.

The following solution was used in electrochemical analysis: 2.5 mmol l^{-1} $K_3Fe(CN)_6$ + 50 mmol l^{-1} KCl. Phosphate-buffered saline (PBS) was prepared with 10 mmol l^{-1} sodium phosphate and 150 mmol l^{-1} sodium chloride and was adjusted to pH 7.0 with 1 N hydrochloric acid. All the solutions were filtered through a 0.22-μm membrane filter and purged with nitrogen for 15 min prior to measurement.

2.2. Surface plasmon resonance experiment

SPR measurement was performed using a cuvette-based Autolab electrochemical surface plasmon resonance (ESPR) instrument (Eco Chemie BV, The Netherlands). The SPR data were recorded with a frequency of 0.5 Hz. The glass side of the sensor disc substrate was attached to the half-cylinder prism with a refractive-index-matching liquid. Upon the gold side of the substrate, a combined electrochemistry–SPR cuvette, equipped with an outlet and a pump to drain out the liquid from the cuvette cell, was mounted. After each step, the cell and disc were washed with ultrapure water three times and SPR data were recorded in the PBS buffer, pH 7.0.

2.3. Preparation of supported lipid bilayer on gold disc

The lipid (DDAB) was dissolved in chloroform in a glass vial. The solvent was evaporated under a pure nitrogen flow. The lipid was resuspended in 10 mmol l^{-1} phosphate buffer, pH 6.0, and then sonicated in an ultrasonic bath until a clear solution was obtained. At this time, the suspended lipid formed unilamellar vesicles. Buffer was added to fix the final lipid concentration (5 mg ml^{-1}).

The sensor disc of the ESPR was used for

fabrication of the supported lipid bilayer. This is a glass disc with a gold film, 50 nm thick, deposited on one side. Before use, the disc was treated with piranha acid (a mixture of concentrated H_2SO_4 and H_2O_2) for several minutes, and then rinsed with ethanol. After thoroughly rinsing with ultrapure water, the disc was mounted on the half-cylinder prism and then the combined electrochemistry–SPR cuvette was mounted on the gold film of the disc.

Prior to use, the surface of the gold film was subjected to cyclic potential sweeps between -0.2 and $+1.5$ V in 1 mol l^{-1} H_2SO_4 until a stable cyclic voltammogram was obtained. Next, the surface was incubated with 1 mmol l^{-1} MPA for 4 h. The solution was then drained out with the pump. The cell was rinsed with water to remove excess acid. At this time, a self-assembled monolayer (SAM) was formed on the gold film. The lipid bilayer was then formed on the SAM layer by the electrostatic adsorption method. The vesicle preparation was added to the cuvette. The surface of the MPA monolayer was negatively charged, and the hydrophilic surface of vesicle was positively charged. The vesicles were adsorbed onto the SAM surface, fused and a lipid bilayer formed, as described by Steinem et al. [17]. After 1 h, the excess solution was drained out with the pump, and the cell and lipid bilayer formed were rinsed with water.

2.4. Electrochemical measurements

Electrochemical experiments were performed in the ESPR cuvette cell (150 μl) coupled to a three-electrode system. The gold film of the ESPR sensor disc was used as the working electrode (diameter 5 mm), an Ag/AgCl electrode (saturated KCl) was the reference electrode and a platinum wire was the counter electrode. Cyclic voltammetry was performed in a 2.5 mmol l^{-1} $K_3Fe(CN)_6$ + 50 mmol l^{-1} KCl solution at a scan rate of 100 mV s^{-1}. The scan range was from -0.2 to $+0.6$ V. Cyclic voltammetry was performed with an Autolab PGSTA-30 digital potentiostat/galvanostat, using GPES 4.9 software for electrochemical measurements (Eco Chemie BV, The Netherlands). For impedance measurement, an FRA module with FRA software 4.9 (Eco Chemie BV) was used. The impedance spectra were recorded within the frequency range of 0.1–100 000 Hz. The amplitude of the applied sine-wave potential in each case was 50 mV, while the DC potential was 0.22 V in the presence of $K_4[Fe(CN)_6]$ and $K_3[Fe(CN)_6]$ as the redox couple.

3. Results and discussion

3.1. Cyclic voltammetric behavior of the lipid bilayer

Cyclic voltammetry has been widely used to characterize self-assembled monolayers and bilayers on solid support surfaces [18–20]. These studies showed that electrochemical reaction involving dissolved redox ions could be strongly suppressed by the presence of organic layers. Fig. 1A shows CV curves of the $K_3[Fe(CN)_6]$ redox probe, solubilized in electrolyte solution, on a bare gold-film electrode (curve a), on the self-assembled monolayer of MPA (curve b) and on the subsequently formed lipid bilayer (curve c). The curve of the bare gold electrode is typical for a diffusion-controlled reversible redox process. The peak current was relatively large due to the large area of the gold film electrode surface. The MPA-modified gold electrode resulted in small peak-to-peak separation and a slight decrease in amperometric response. However, upon the formation of the lipid bilayer on the gold support, a significant change was observed. The large decrease in the amperometric response and an increase in the peak-to-peak separation indicated that the interfacial electron-transfer between the redox probe and the gold surface was mostly blocked. This implied that a lipid bilayer had been successfully formed on the MPA-modified gold film electrode.

3.2. Electrochemical impedance behavior of the lipid bilayer

It is well known that impedance spectroscopy is an effective method for probing the interfacial properties of modified electrodes, and is often used for understanding chemical transformations and processes associated with conductive supports

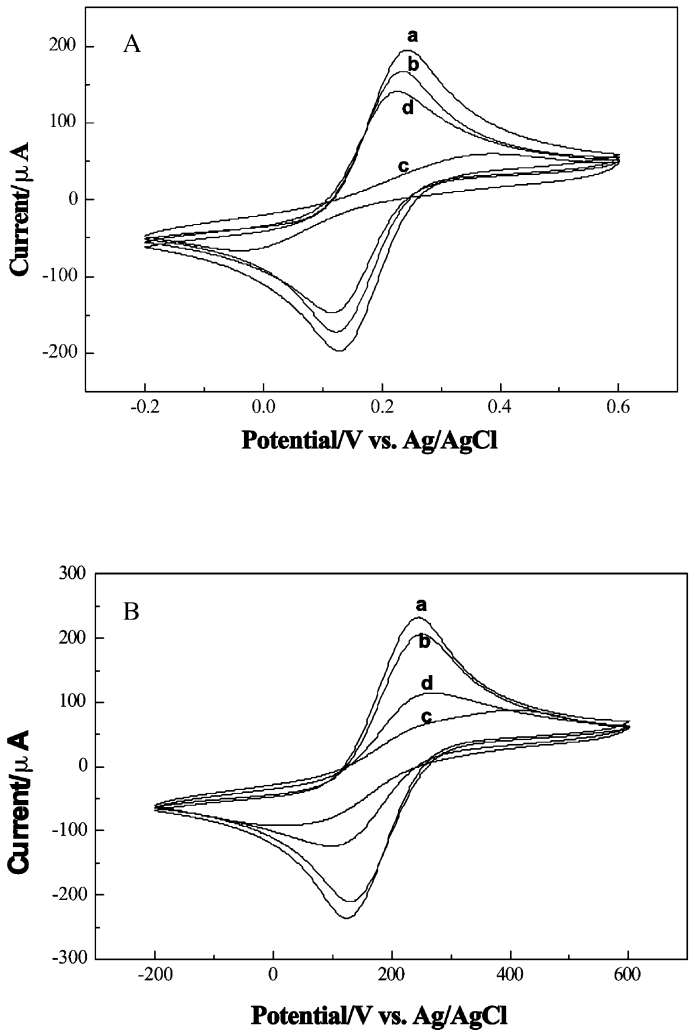

Fig. 1. Cyclic voltammogram recorded in an $K_3Fe(CN)_6$ solution when the measuring film electrode was: (A) bare gold; (B) gold modified with MPA; (c) as in (b) with additional modification with lipid vesicles; (d) as in (c) after incubation with chitosan. Chitosan concentration was (A) 250; and (B) 50 μg ml^{-1} in PBS buffer (0.01 mol l^{-1}, pH 7.0, 0.15 mol l^{-1} NaCl).

[21,22,20]. The adsorption and desorption of insulting materials on conductive supports is anticipated to alter the interfacial electron-transfer features (capacitance and resistance) at the electrode surface. Therefore, in the present work, the impedance technique was also used as an electrochemical sensing method as well as CV.

Fig. 2 shows the results of Faradic impedance spectroscopy presented as Nyquist plots (Z_{im} vs. Z_{re}) on a bare gold electrode (curve a), an MPA-modified electrode (curve b) and a lipid bilayer formed in the presence of the redox probe $Fe(CN)_6^{4-/3-}$ measured at their formal potential (inset). The impedance spectra followed the theoretical shapes, including a semicircle portion observed at higher frequencies, which corresponds to the electron transfer-limited process, followed by a linear part, characteristic of the lower frequency attributable to diffusionally limited electron transfer. The semicircle diameter corresponded to

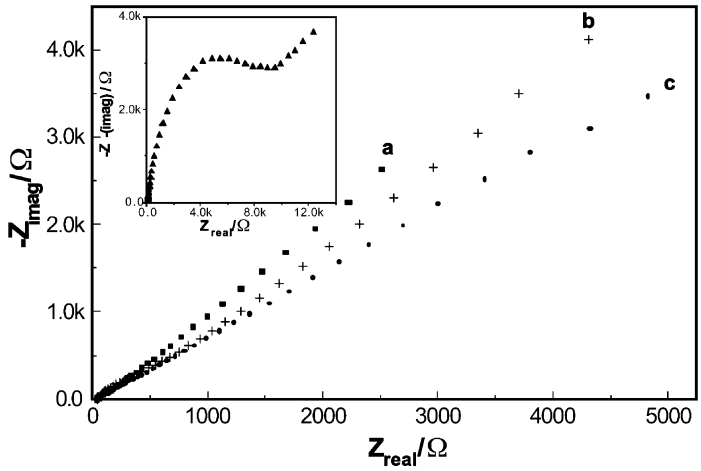

Fig. 2. Nyquist diagram for the Faradic impedance measurement in 2.5 mmol l^{-1} $Fe(CN)_6^{4-/3-}$ + 0.25 mol. l^{-1} KCl solution on: (a) bare gold surface; (b) MPA-modified gold surface; and (c) BLM surface after incubation with 250 μg ml^{-1} chitosan. The inset shows the curve for the MPA-modified surface after incubation with lipid vesicles.

the electron transfer resistance at the electrode surface (R_{ct}). It could be observed that the diameter of semicircle at high frequency increased upon the formation of SAM and the lipid bilayer on the electrode surface. Fox example, for the bare electrode R_{et} = 37 Ω (Fig. 2, curve a), R_{et} = 144 Ω (Fig. 2, curve b) upon SAM of MPA, whereas R_{et} increased to 9700 Ω (Fig. 2, inset) on subsequent formation of the lipid bilayer. The reason might be that when the lipid bilayer formed, the tightly arranged lipid layer almost blocked the redox probe to the electrode surface.

From the above, it could be confirmed that the lipid bilayer was successfully formed on the gold surface. The impedance spectroscopy data agreed with the cyclic voltammograms observed.

3.3. Surface plasmon resonance analysis

A SPR sensorgram of the lipid bilayer formation is shown in Fig. 3a. The incubation of vesicles on

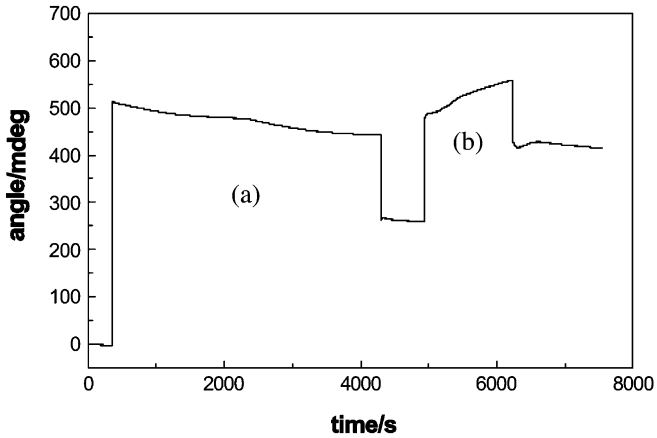

Fig. 3. SPR sensorgram of binding of vesicles on MPA-modified surface and the interaction of the lipid bilayer formed with chitosan: (a) adsorption of vesicles; and (b) addition of chitosan to the lipid bilayer.

MPA modified surface produced a 0.280° shift of the SPR angle. According to a previous report [23], complete coverage of the surface with a phosphatidylcholine (PC) monolayer caused a 2200 RU response increase in a BIAcore instrument, which corresponded to a surface lipid density of 2.0 ng mm^{-2} (0.92 ± 0.05 pg mm^{-2} RU^{-1}). We may deduce that formation of a lipid bilayer may cause a change of 4400 RU or a surface lipid density of 4.0 ng mm^{-2}. In an Autolab SPR instrument, a surface lipid density change of 1.0 ng mm^{-2} produces a 0.132° SPR angle shift. In the present study, a 0.280° shift corresponding to a surface lipid density of 2.1 ng mm^{-2} was observed after incubation of the vesicles on the MPA surface. The MW of the lipid used in the present study (DDAB) was half of that of PC. Thus, the surface lipid density of 2.1 ng mm^{-2} in our study corresponded to a lipid bilayer formed on the gold surface.

3.4. Interaction of chitosan with lipid bilayer

A chitosan solution of 250 μg ml^{-1} in PBS (0.01 mol l^{-1}, pH 7.0, 0.15 mol l^{-1} NaCl) was applied to the lipid bilayer formed and incubated for 15 min. The solution was then drained out. After rinsing with water, the lipid bilayer was characterized by SPR and electrochemical methods. The cyclic voltammetry behavior (Fig. 1A, curve d) significantly changed compared with the undisturbed lipid bilayer. The large increase in the amperometric response and an increase in the peak-to-peak separation indicated that the integrity of the lipid bilayer might have been disturbed. The impedance spectroscopy is shown in Fig. 2, curve c. The R_{et} value decreased to 324 Ω, indicating that the barrier of the redox probe to the surface was disrupted.

In the absence of chitosan, the lipid bilayer served as a rather effective barrier against electron tunneling. The results presented above showed that the addition of chitosan caused the formation of some transmembrane channels for the redox probe across the lipid bilayer. The SPR analysis of the interaction is shown in Fig. 3b. The addition of chitosan caused a 0.150° shift in the SPR angle, indicating that chitosan was adsorbed to the surface.

Chitosan is a basic polymer with an intrinsic pK_a value of ~6.5 (primary amines), independent of the degree of deacetylation [24]. This suggests that chitosan is protonated and positively charged at and below pH 7 [9]. In this study, the existence of a DDAB bilayer was proved by electrochemical methods and the SPR technique. Although physically adsorbed chitosan may promote the redox probe $Fe(CN)6^{4-/3-}$ to the surface because of the positive charge on chitosan, we might exclude this possibility due to electrostatic repulsion between chitosan and the positively charged lipid-bilayer surface. For the only case in which chitosan penetrated into the lipid bilayer, the integrity of the lipid bilayer was disrupted, as shown by Chan et al. [25]. The chitosan-induced destabilization was also confirmed by a higher initial rate of quinine release from a chitosan/liposome complex compared with pure liposome [26]. We think that electrostatic repulsion between the protonated amino groups of chitosan and the positively charged surface of the lipid bilayer played an important role in the interaction. The hydrophobic interaction between the *N*-acetyl group on the chitosan backbone (degree of acetylation was 10%) and the hydrophobic core of the lipid bilayer was another driving force, as described by Chan and co-workers [25,27]. The *N*-acetyl group on the chitosan backbone imparted hydrophobic properties to the lipid bilayer. The LMW chitosan used in the present study was soluble in PBS buffer at neutral pH, at which chitosan with a large molecular weight is insoluble. The high solubility of chitosan used in the present study may compensate for the relatively weak electrostatic and hydrophobic effect. A combined electrostatic–hydrophobic driving force caused destabilization of the membrane. From the discussion above, we might conclude that changes in the cyclic voltammograms and impedance spectra were due to the formation of some 'defects' on the lipid bilayer as a result of the interaction between chitosan and the lipid.

It was reported that chitosan significantly suppressed the enthalpy of the gel–crystalline transition of a phospholipid bilayer and caused serious disorganization of the ordered bilayer structure in

a concentration-dependent manner [25]. Ranaldi et al. [28] found that chitosan might increase the tight junction permeability in the human intestinal Caco-2 cell line. The effect was in a concentration-dependent fashion. The effect of LMW chitosan on a lipid bilayer in our study also appeared to be concentration-dependent. A chitosan solution of 50 $\mu g\ ml^{-1}$ in PBS buffer was applied to the lipid bilayer as described above. CV curves are shown in Fig. 1B. The increase in the amperometric response was relatively smaller than that with chitosan solution of 250 $\mu g\ ml^{-1}$, as shown in Fig. 1a. The chitosan sample with higher concentration may have a relatively stronger action on the lipid bilayer.

There have been very few studies on the interaction between chitosan and biomembranes using electrochemical methods and the SPR technique. The results obtained in our study are of great significance for pharmaceutical applications of chitosans. Most chitosans used in previous studies were of large molecular weight and should be used at acidic pH. At neutral pH, they are insoluble, and are therefore ineffective. An increase in molecular weight may increase the risk of toxicity, and the poor solubility at neutral pH limits their uses. LMW chitosans were proved to be neither toxic nor hemolytic and could be administered intravenously. It is critical to investigate the interaction between LMW chitosan and cell membranes under physiological pH conditions. As a gene delivery carrier, chitosan increased the transfection efficiency of complexed DNA when the target cells were incubated with nanoparticles in the presence of chitosan [10]. Chitosan and its derivatives, in either free amino or acid forms, were used as absorption enhancers of drugs [29–32]. Our results showed that LMW chitosan could destabilize the lipid bilayer at neutral pH, and thus may provide an explanation for these studies. Its high solubility and low toxicity expand its use as a drug excipient. In many pharmaceutical applications, chitosans can disturb the integrity of the cell membrane, and thus promote the absorption of drugs and DNA. Since chitosans exhibit antibacterial and antifungal activity, they have attracted much attention as potential food preservatives [11]. Chitosans could sensitize harmful bacteria to other potentially inhibitory substances by facilitating their entry into the bacterial cells. They could also change the permeability of the cell membrane and even disrupt it, resulting in the leakage of cell constituents.

4. Conclusions

In this paper, a solid supported lipid bilayer was successfully formed on the gold surface of an ESPR sensor disc by fusion of positively charged vesicles on an oppositely charged self-assembled monolayer of MPA. We characterized the formation of the lipid bilayer and studied its interaction with low-molecular-weight chitosan with cyclic voltammetry, electrochemical impedance spectroscopy and surface plasmon resonance. The chitosan induced the formation of a mass-transfer channel in the lipid bilayer at neutral pH. The results gave direct evidence of the disturbance effect of LMW chitosan on cell membranes. The high solubility and low toxicity of LMW chitosan and its bioactivities at neutral pH can expand the use of chitosan in the pharmaceutical and food industries.

Acknowledgments

We thank the National Natural Science Foundation of China (NSFC) for support of this work (Grant No 20075027).

References

[1] S. Sabnis, L.H. Block, Chitosan as an enabling excipient for drug delivery systems I. Molecular modifications, Int. J. Biol. Macromol. 27 (2000) 181–186.
[2] P. Artursson, T. Lindmark, S.S. Davis, L. Illum, Effect of chitosan on the permeability of monolayer of intestinal epithelial cells (Caco-2), Pharm. Res. 11 (1994) 1358–1361.
[3] V. Dodane, M.A. Khan, J.R. Merwin, Effect of chitosan on epithelial permeability and structure, Int. J. Pharm. 182 (1999) 21–32.
[4] Z. Jia, D. Shen, W. Xu, Synthesis and antibacterial activities of quaternary ammonium salt of chitosan, Carbohydrate Res. 333 (2001) 1–6.
[5] I.M. Helander, E.L. Nurmiaho-Lassila, R. Ahvenainen, J. Rhoades, S. Roller, Chitosan disrupts the barrier properties of the outer membrane of Gram-negative bacteria, Int. J. Food Microbiol. 71 (2001) 235–244.
[6] K. Roy, H.Q. Mao, S.K. Huang, K.W. Leong, Oral gene delivery with chitosan–DNA nanoparticles generates

immunologic protection in a murine model of peanut allergy, Nat. Med. 5 (1999) 387–391.
[7] V.L. Truong-Le, S.M. Walsh, E. Schweiberg, et al., Gene transfer by DNA–gelatin nanospheres, Arch. Biochem. Biophys. 361 (1999) 47–56.
[8] K.W. Leong, H.Q. Mao, V.L. Truong-Le, K. Roy, S.M. Walsh, J.T. August, DNA–polycation nanospheres as non-viral gene delivery vehicles, J. Controlled Release 23 (1998) 153–159.
[9] T. Sato, T. Ishii, Y. Okahata, In vitro gene delivery mediated by chitosan. Effect of pH, serum, and molecular mass of chitosan on the transfection efficiency, Biomaterials 22 (2001) 2075–2080.
[10] H.Q. Mao, K. Roy, V.L. Truong-Le, et al., Chitosan–DNA nanoparticles as gene carriers: synthesis, characterization and transfection efficiency, J. Controlled Release 70 (2001) 399–421.
[11] S.C.W. Richardson, H.V.J. Kolbe, R. Duncan, Potential of low molecular mass chitosan as a DNA delivery system: biocompatibility, body distribution and ability to complex and protect DNA, Int. J. Pharm. 178 (1999) 231–243.
[12] G. Brink, L. Schmitt, R. Tampe, E. Sackmann, Self-assembly of covalently anchored phospholipid-supported membrane by use of DODA-Suc-NHS-lipids, Biochim. Biophys. Acta 1196 (1994) 227–230.
[13] T. Stora, Z. Dienes, H. Vogel, C. Duschl, Histidine-tagged amphiphiles for the reversible formation of lipid bilayer aggregates on chelator-functionalized gold surface, Langmuir 16 (2000) 5471–5478.
[14] O. Pierrat, C. Bourdillon, J. Moirous, J. Laval, Enzymatic electrocatalysis studies of *Escherichia coli* pyruvate oxidase, incorporated into a biomimetic supported bilayer, Langmuir 14 (1998) 1692–1696.
[15] O. Pierrat, N. Lechat, C. Bourdillon, J. Laval, Electrochemical and surface plasmon resonance characterization of the step-by-step self-assembly of a biomimetic structure onto an electrode surface, Langmuir 13 (1997) 4112–4118.
[16] L.M. Willams, S.D. Evans, T.M. Flynn, et al., Kinetics of the unrolling of small unilamellar phospholipid vesicles onto self-assembled monolayer, Langmuir 13 (1997) 751–757.
[17] C. Steinem, A. Janshoff, J. Wegener, et al., Impedance and shear wave resonance analysis of ligand–receptor interactions at functionalized surfaces and of cell monolayer, Biosens. Bioelectron. 12 (1997) 787–808.
[18] F. Auer, B. Sellergren, A. Swietlow, A. Offenhauser, Self-assembled layers of bisbenzamidines on gold, Langmuir 16 (2000) 5936–5944.
[19] S. Chen, K. Huang, Ion-induced interfacial dynamics of phospholipid monolayers, Anal. Chem. 72 (2000) 2949–2956.
[20] Z. Wu, J. Tang, Z. Cheng, X. Yang, E. Wang, Ion channel behavior of supported lipid bilayer membrane on a glass carbon electrode, Anal. Chem. 72 (2000) 6030–6033.
[21] R.P. Janek, W.R. Fawcett, A. Ulman, Impedance spectroscopy of self-assembled monolayers on Au(111): sodium ferrocyanide charge transfer at modified electrodes, Langmuir 14 (1998) 3011–3018.
[22] Z. Cheng, E. Wang, X. Yang, Capacitive detection of glucose using molecular imprinted polymers, Biosens. Bioelectron. 16 (2001) 179–183.
[23] M.A. Cooper, A.C. Try, J. Carroll, D.J. Ellar, D.H. Williams, Surface plasmon resonance analysis at a supported lipid bilayer, Biochim. Biophys. Acta 1373 (1998) 101–111.
[24] N.G.M. Schipper, K.M. Vårum, P. Artusson, Chitosan as absorption enhancers of poorly absorbable drugs. 1. Influence of molecular weight and degree of acetylation on drug transport across human intestinal epithelial (Caco-2) cells, Pharm. Res. 13 (1996) 1686–1692.
[25] V. Chan, H. Mao, K.W. Leong, Chitosan-induced perturbation of dipalmitoyl-*sn*-glycero-3-phosphocholine membrane bilayer, Langmuir 17 (2001) 3749–3756.
[26] I. Henriksen, S.R. Vagen, S.A. Sande, G. Smistad, J. Karslen, Interaction between liposomes and chitosan II: effect of selected parameters on aggregation and leakage, Int J. Pharm. 146 (1997) 193–203.
[27] N. Fang, V. Chan, H.Q. Mao, K.W. Leong, Interactions of phospholipid bilayer with chitosan: effect of molecular weight and pH, Biomacromolecules 2 (2001) 1161–1168.
[28] G. Ranaldi, I. Marigliano, I. Vespignani, G. Perozzi, Y. Sambuy, The effect of chitosan on tight junction permeability in the human intestinal Caco-2 cell line, J. Nutr. Biochem. 13 (2002) 157–167.
[29] P. Tengamnuay, A. Sahamethapat, A. Sailasuta, A.K. Mitra, Chitosan as nasal absorption enhancers of peptides: comparison between free amine chitosans and soluble salts, Int. J. Pharm. 197 (2000) 53–67.
[30] N.G.M. Schipper, K.M. Vårum, P. Stenberg, G. Qcklind, H. Lennernas, P. Artusson, Chitosan as absorption enhancers of poorly absorbable drugs 3: influence of mucus on absorption enhancement, Eur. J. Pharm. Sci. 8 (1999) 335–343.
[31] A.F. Kotze, H.L. Luebon, B.J. De Leeuw, B.G. De Boer, J.C. Verhoef, H.E. Junginger, Comparison of the effect of different chitosan salts and *N*-trimethyl chitosan chloride on the permeability of intestinal epithelial cells (Caco-2), J. Controlled Release 51 (1998) 35–46.
[32] P. He, S.S. Davis, L Illum, In vitro evaluation of the mucoadhesive properties of chitosan microspheres, Int. J. Pharm. 166 (1998) 75–88.